NUMERICAL SIMULATION OF THE TRANSONIC LAMINAR FLOW IN AIRFOILS WITH PITCHING AND PLUNGING MOTION

Rúdner Lauterjung Queiroz
Universidade de Brasília, ENM – FT – UnB, Campus Universitário Darcy Ribeiro, Asa Norte, 70910-900, Brasília, DF, Brasil
rudner@gmail.com

Jean Rafael Jalowitzki
Universidade de Brasília, ENM – FT – UnB, Campus Universitário Darcy Ribeiro, Asa Norte, 70910-900, Brasília, DF, Brasil
j0052019@aluno.unb.br

Roberto Francisco Bobenrieth Miserda
Universidade de Brasília, ENM – FT – UnB, Campus Universitário Darcy Ribeiro, Asa Norte, 70910-900, Brasília, DF, Brasil
rfbm@unb.br

Abstract. *The objective of this work is the numerical simulation and comparison between imposed plunging and pitching motions for a NACA 0012 airfoil in a transonic laminar flow. The system of equations is written using a non-inertial frame of reference that is fixed to the plunging or pitching airfoil. The effect of these motions is accounted by introducing pseudo-force and pseudo-work terms in the right-hand side of the momentum and energy equations, respectively. The compressible Navier-Stokes equations are numerically solved using a finite volume discretization in combination with the skew-symmetric form of Ducros' fourth-order numerical scheme for the flux calculations, while the time marching process is achieved using a third-order Runge-Kutta scheme. The linear amplitude of the plunging motion, as well as the angular amplitude of the pitching motion, is imposed as sinusoidal in time, and for all cases studied, the plunging or pitching frequency corresponds to the simulated vortex-emission frequency of the static airfoil at the same angle of attack. In order to compare the two types of motions, for the two cases, the maximum velocity of the airfoil's leading edge is the same. From a system dynamics point of view, the system response to the pitching motion is different when compared to the response to the plunging motion. For the first case, the system response is quasi-linear and in the second case, the response is a non-linear.*

Keywords*: transonic flow, laminar flow, pitching motion, plunging motion, NACA 0012*

1. Introduction

This work is aimed at the numerical simulation of the strong vortex-shock interaction that arises in the transonic flow over NACA 0012 airfoil in laminar regime, submitted to pitching and plunging motions. This kind of interaction is typical of the unsteady aerodynamics of bodies in transonic flows, directly connected to limit cycle oscillations in transonic flows, flutter and dynamic stall phenomena, of high interest in the aerospace sciences. The complex nature of these interactions demands numerical methods with shock-capturing schemes to obtain meaningful results, and in the case of pitching and plunging motions, a modified set of governing equations in order to simulate the oscillations of the body.

Some examples of related methodologies presented in recent works are the unsteady Euler method for non-moving cartesian grids coupled with integral boundary-layer method for the prediction of flutter (Zhang, Yang and Liu, 2005), the kinetic flux-vector splitting scheme on moving grids for solving the unsteady Euler equations around oscillating bodies (Krishnamurthy, Sarma and Deshpande, 2004), and the downwash weighting method for approximating the non-linear behavior of transonic flows (Silva, Mello and Azevedo, 2004). The compressible Navier-Stokes equations, modified in this work using the concept of pseudo-forces and pseudo-work in order to represent the oscillation of the airfoil from a non-inertial frame of reference, are solved using Ducros' fourth-order skew-symmetric scheme for calculating the fluxes in a finite-volume discretization in conjunction with a third-order Runge-Kutta time-marching method, as proposed by Bobenrieth Miserda and Mendonça (2005). Experimental results for high Reynolds numbers are found for dynamic pitching motion in subsonic flow (Tolouei *et al.*, 2004) and transonic flow (Hillenherms, Schröder and Limberg, 2001).

2. Methodology

In this work, the system of equations is written using a non-inertial frame of reference that is fixed to the plunging or pitching airfoil. The effect of these motions is accounted by a pseudo-force term in the right-hand side of the momentum equation that acts as a body force (Batchelor, 1983). In similar manner, the work done by this pseudo-force is accounted by a pseudo-work term in the right-hand side of the energy equation. With these considerations, the nondimensional form of the Navier-Stokes equations can be written as:

$$\frac{\partial \rho}{\partial t}+\frac{\partial}{\partial x_i}(\rho u_i)=0 \tag{1}$$

$$\frac{\partial}{\partial t}(\rho u_i)+\frac{\partial}{\partial x_j}(\rho u_i u_j)=-\frac{\partial p}{\partial x_i}+\frac{\partial \tau_{ij}}{\partial x_j}+f_i \tag{2}$$

$$\frac{\partial}{\partial t}(\rho e_T)+\frac{\partial}{\partial x_i}(\rho e_T u_i)=-\frac{\partial}{\partial x_i}(p u_i)+\frac{\partial}{\partial x_i}(\tau_{ij} u_j)-\frac{\partial q_{x_i}}{\partial x_i}+f_i u_i \tag{3}$$

All the variables are in nondimensional form and have their usual meaning, i.e., ρ is the density, t is the temporal coordinate, x_i is the i-direction spatial coordinate, u_i is the i-direction component of the velocity vector, p is the pressure, τ_{ij} denotes the viscous stress tensor, e_T is the total energy per unit of mass, q_{xi} is the heat-flow density in the i-direction and f_i is the pseudo-force due to the plunging or pitching motion.

The nondimensional form of the flow variables and properties are defined as

$$\begin{aligned} &x_i=\frac{x_i^*}{c^*},\quad u_i=\frac{u_i^*}{U_\infty^*},\quad t=\frac{t^*}{c^*/U_\infty^*},\quad p=\frac{p^*}{\rho_\infty^*\left(U_\infty^*\right)^2},\quad \rho=\frac{\rho^*}{\rho_\infty^*},\quad e_T=\frac{e_T^*}{\left(U_\infty^*\right)^2},\\ &\mu=\frac{\mu^*}{\mu_\infty^*},\quad e=\frac{e^*}{\left(U_\infty^*\right)^2},\quad e_k=\frac{e_k^*}{\left(U_\infty^*\right)^2},\quad c_v=\left[\frac{T_\infty^*}{\left(U_\infty^*\right)^2}\right]c_v^*,\quad T=\frac{T^*}{T_\infty^*}, \end{aligned} \tag{4}$$

where the asterisk denotes dimensional quantities, c^* is the chord of the airfoil, μ^* is the dynamic viscosity, T^* is the temperature. U^*_∞, T^*_∞, ρ^*_∞ and μ^*_∞ are, respectively, the velocity, temperature, density and dynamic viscosity of the undisturbed flow. The nondimensional viscous stress tensor is given by

$$\tau_{ij}=\frac{1}{\mathrm{Re}}\left(\mu S_{ij}\right)=\frac{1}{\mathrm{Re}}\left\{\mu\left[\left(\frac{\partial u_i}{\partial x_j}+\frac{\partial u_j}{\partial x_i}\right)-\frac{2}{3}\delta_{ij}\frac{\partial u_k}{\partial x_k}\right]\right\} \tag{5}$$

where δ_{ij} is the Kronecker delta. The Reynolds number is defined as

$$\mathrm{Re}=\frac{\rho_\infty^* U_\infty^* c^*}{\mu_\infty^*}. \tag{6}$$

Defining e as the nondimensional internal energy per unit of mass, e_k as the nondimensional kinetic energy per unit of mass and c_v as the nondimensional specific heat at constant volume, the total energy is given by the sum of the internal and kinetic specific energy as

$$e_T=e+e_k=c_v T+\frac{u_i u_i}{2} \tag{7}$$

and the nondimensional heat-flux density is

$$q_{x_i}=-\frac{\mu}{(\gamma-1)M^2\,\mathrm{Re}\,\mathrm{Pr}}\left(\frac{\partial T}{\partial x_i}\right) \tag{8}$$

where the M and Pr are the Mach and the Prandtl numbers, respectively, and are defined as

$$M=\frac{U_\infty^*}{\sqrt{\gamma R^* T_\infty^*}},\qquad \mathrm{Pr}=\frac{c_p^*}{k_\infty^*}\mu_\infty^* \tag{9}$$

where γ is the specific heat ratio, R^* is the specific gas constant, $c_p{}^*$ is the specific heat at constant pressure and $k_\infty{}^*$ is thermal conductivity of the undisturbed flow.

In this work, the Prandtl number is considered a constant with the value $\mathrm{Pr} = 0.72$. For a thermally and calorically perfect gas, the nondimensional equation of state can be written as

$$p = (\gamma - 1)\rho e \tag{10}$$

and

$$T = \frac{\gamma M^2 p}{\rho} \tag{11}$$

The nondimensional molecular viscosity is obtained using Sutherland's formula, where C_1 and C_2 are the nondimensional first and second gas constants,

$$\mu = C_1 \frac{T^{3/2}}{T + C_2}, \qquad C_1 = \left[\frac{\left(T_\infty^*\right)^{1/2}}{\mu_\infty^*} \right] C_1^*, \qquad C_2 = \frac{C_2^*}{T_\infty^*}. \tag{12}$$

The objective of this work is to make a comparison between the effect of the plunging and pitching motions over the resulting aerodynamic forces. The pseudo-force f_i, that appears in Eqs. (2) and (3), accounts for the two types of motion when the Navier-Stokes equations are written for a non-inertial frame or reference. When the imposed motion is a plunging one and its linear amplitude is sinusoidal in time, the components of the pseudo-force, f_i, are given by

$$f_i = \frac{1}{2} \rho A_i \omega_i^2 \sin(\omega_i t) \tag{13}$$

The nondimensional maximum amplitude, A_i, and angular frequency, ω_i, of the plunging motion are defined as

$$A_i = \frac{A_i^*}{c^*}, \qquad \omega_i = \frac{\omega_i^*}{U_\infty^* / c^*}. \tag{14}$$

On the other hand, when the imposed motion is a pitching one, and its angular amplitude is sinusoidal in time, the components of the pseudo-force, f_i, are

$$f_i = -\rho \left[2\left(\varepsilon_{ijk} \Omega_j u_k\right) + \left(\varepsilon_{jik} \varepsilon_{jpm} \Omega_p r_m \Omega_k\right) + \left(\varepsilon_{ijk} \frac{d\Omega_j}{dt} r_k \right) \right], \tag{15}$$

where ε_{ijk} is the Levi-Civita multiplier, r_i is the position vector relative to the pitching frame of reference, Ω_i is the angular velocity and $d\Omega_i / dt$ is the angular acceleration. This velocity and acceleration are given by

$$\Omega_i(t) = -\frac{1}{2} \omega_i \beta_i \cos(\omega_i t), \qquad \frac{d\Omega_i}{dt} = \frac{1}{2} \omega_i^2 \beta_i \sin(\omega_i t), \tag{16}$$

where β_i is the maximum angular amplitude of the motion and ω_i is the nondimensional angular frequency of the pitching motion, defined in the same manner as Eq. (14). It is important to note that the first right-hand side term of Eq. (15) is the Coriolis acceleration, the second term is the centrifugal acceleration and the last term is the tangential acceleration, due to the angular acceleration.

The boundary conditions at the wall of the two-dimensional airfoil are a no-slip condition for the velocity field, an adiabatic wall for the temperature field and a null gradient in the normal direction at the wall for the pressure field.

Since the geometry of interest is a two-dimensional airfoil and the flow around it is laminar, the two-dimensional form of the Navier-Stokes equations is used. In order to numerically solve these equations using a finite volume approach associated with a fixed grid, Eqs. (1), (2) and (3) are written in the following vector form (Anderson, 1983):

$$\frac{\partial \mathbf{U}}{\partial t} + \frac{\partial \mathbf{E}}{\partial x} + \frac{\partial \mathbf{F}}{\partial y} = \mathbf{R} \tag{17}$$

where **U** is the nondimensional conservative-variables vector, **E** and **F** are the nondimensional flux vectors. These vectors are given by

$$\mathbf{U}=\begin{bmatrix}\rho\\ \rho u\\ \rho v\\ \rho e_T\end{bmatrix},\quad \mathbf{E}=\begin{bmatrix}\rho u\\ \rho u^2+p-\tau_{xx}\\ \rho uv-\tau_{xy}\\ (\rho e_T+p)u-u\tau_{xx}-v\tau_{xy}+q_x\end{bmatrix},\quad \mathbf{F}=\begin{bmatrix}\rho v\\ \rho vu-\tau_{xy}\\ \rho v^2+p-\tau_{yy}\\ (\rho e_T+p)v-u\tau_{xy}-v\tau_{yy}+q_y\end{bmatrix}, \tag{18}$$

where u and v are, respectively, the nondimensional component of the velocity vector in the x-direction and y-direction.

In this work, the plunging motion of the airfoil is imposed in the y-direction, and consequently, for this case the nondimensional **R** vector, that is associated with the plunging or pitching motion, is

$$\mathbf{R}=\begin{bmatrix}0\\ 0\\ \frac{1}{2}\rho A_y\omega^2\sin(\omega_y t)\\ \frac{1}{2}\rho A_y\omega^2\sin(\omega_y t)v\end{bmatrix}. \tag{19}$$

For the case of a sinusoidal pitching motion in the x-y plane, $\Omega_x=\Omega_y=0$, and consequently, the **R** vector is given by

$$\mathbf{R}=\begin{bmatrix}0\\ \rho\left(2\Omega_z v+\Omega_z^2 r_x+\frac{d\Omega_z}{dt}r_y\right)\\ -\rho\left(2\Omega_z u-\Omega_z^2 r_y+\frac{d\Omega_z}{dt}r_x\right)\\ \rho\left(2\Omega_z v+\Omega_z^2 r_x+\frac{d\Omega_z}{dt}r_y\right)u-\rho\left(2\Omega_z u-\Omega_z^2 r_y+\frac{d\Omega_z}{dt}r_x\right)v\end{bmatrix}, \tag{20}$$

where the z-direction angular velocity and acceleration are

$$\Omega_z(t)=-\frac{1}{2}\omega_z\beta\cos(\omega_z t),\qquad \frac{d\Omega_z}{dt}=\frac{1}{2}\omega_z^2\beta\sin(\omega_z t), \tag{21}$$

Defining the flux tensor Π as

$$\Pi=\mathbf{E}\otimes\mathbf{i}+\mathbf{F}\otimes\mathbf{j} \tag{22}$$

where **i** and **j** are unit vectors in the x-direction and y-direction. Eq. (17) can be rewritten as

$$\frac{\partial\mathbf{U}}{\partial t}+\nabla\cdot\Pi=\mathbf{R} \tag{23}$$

Integrating the above equation over the control volume V, and applying the divergence theorem to the first term of right-hand side results

$$\frac{\partial}{\partial t}\int_V\mathbf{U}\,dV=-\int_V(\nabla\cdot\Pi)dV+\int_V\mathbf{R}\,dV=-\int_S(\Pi\cdot\mathbf{n})dS+\int_V\mathbf{R}\,dV \tag{24}$$

Defining the volumetric mean of vectors **U** and **R** in the control volume V as

$$\overline{\mathbf{U}}\equiv\frac{1}{V}\int_V\mathbf{U}\,dV,\qquad \overline{\mathbf{R}}\equiv\frac{1}{V}\int_V\mathbf{R}\,dV, \tag{25}$$

The upper bar means volumetric mean of the variable. Eq. (24) is written as

$$\frac{\partial \overline{\mathbf{U}}}{\partial t} = -\frac{1}{V}\int_S (\Pi \cdot \mathbf{n}) dS + \overline{\mathbf{R}} \tag{26}$$

For the volume (i, j), the first-order approximation of the temporal derivative is given by

$$\left(\frac{\partial \overline{\mathbf{U}}}{\partial t}\right)_{i,j} = \frac{\Delta \overline{\mathbf{U}}_{i,j}}{\Delta t} + O(\Delta t) \tag{27}$$

and the temporal approximation of Eq. (26) for a quadrilateral and two-dimensional control volume is

$$\Delta \overline{\mathbf{U}}_{i,j} = -\frac{\Delta t}{V_{i,j}}\left[\int_{S_{i+1/2}} (\Pi \cdot \mathbf{n}) dS + \int_{S_{i-1/2}} (\Pi \cdot \mathbf{n}) dS + \int_{S_{j+1/2}} (\Pi \cdot \mathbf{n}) dS + \int_{S_{j-1/2}} (\Pi \cdot \mathbf{n}) dS\right] + \Delta t \overline{\mathbf{R}} \tag{28}$$

where $S_{i+1/2}$ is the common surface between volume (i, j) and volume $(i+1, j)$, $\mathbf{n}$ is the normal unit vector, Δt is the nondimensional time step. Defining

$$\mathcal{F}\left(\overline{\mathbf{U}}\right)_{i,j} = (\Pi \cdot \mathbf{S})_{i+1/2} + (\Pi \cdot \mathbf{S})_{i-1/2} + (\Pi \cdot \mathbf{S})_{j+1/2} + (\Pi \cdot \mathbf{S})_{j-1/2} \tag{29}$$

the spatial approximation of Eq. (28) is

$$\Delta \overline{\mathbf{U}}_{i,j} = -\frac{\Delta t}{V_{i,j}}\left[\mathcal{F}\left(\overline{\mathbf{U}}\right)_{i,j} - \mathcal{D}\left(\overline{\mathbf{U}}\right)_{i,j}\right] + \Delta t \overline{\mathbf{R}} \tag{30}$$

where $\mathcal{D}\left(\overline{\mathbf{U}}\right)_{i,j}$ is an artificial dissipation. It is important to note that Eq. (30) is a spatial approximation of Eq. (28) because tensor Π is considered constant over each of the four control surfaces that define the control volume. In order to calculate $\mathcal{F}\left(\overline{\mathbf{U}}\right)_{i,j}$, the flux of tensor Π trough the control surfaces must be calculated. The explicit form of this calculation as well as the implementation of the artificial dissipation, $\mathcal{D}\left(\overline{\mathbf{U}}\right)_{i,j}$, is given by Bobenrieth Miserda and Mendonça (2005).

In order to advance Eq. (30) in time, a third-order Runge-Kutta is used as proposed by Shu (Yee, 1997). This yield to

$$\overline{\mathbf{U}}^1 = \overline{\mathbf{U}}^n - \frac{\Delta t}{V_{i,j}}\left[\mathcal{F}\left(\overline{\mathbf{U}}^n\right) - \mathcal{D}\left(\overline{\mathbf{U}}^n\right)\right] + \Delta t \overline{\mathbf{R}}^n, \tag{31}$$

$$\overline{\mathbf{U}}^2 = \frac{3}{4}\overline{\mathbf{U}}^n + \frac{1}{4}\overline{\mathbf{U}}^1 - \frac{1}{4}\left\{\frac{\Delta t}{V_{i,j}}\left[\mathcal{F}\left(\overline{\mathbf{U}}^1\right) - \mathcal{D}\left(\overline{\mathbf{U}}^1\right)\right] + \Delta t \overline{\mathbf{R}}^1\right\}, \tag{32}$$

$$\overline{\mathbf{U}}^{n+1} = \frac{1}{3}\overline{\mathbf{U}}^n + \frac{2}{3}\overline{\mathbf{U}}^2 - \frac{2}{3}\left\{\frac{\Delta t}{V_{i,j}}\left[\mathcal{F}\left(\overline{\mathbf{U}}^2\right) - \mathcal{D}\left(\overline{\mathbf{U}}^2\right)\right] + \Delta t \overline{\mathbf{R}}^2\right\}. \tag{33}$$

As used in this work, the numerical method is fourth-order accurate in space and third-order accurate in time.

3. Results

In order to compare the effects of the plunging and pitching motions, two cases are studied. For both cases, the Mach number is 0.8, the Reynolds number is 10^4 and the mean angle of attack is 7^o. The angular frequencies for the plunging motion, ω_y, and for the pitching motion, ω_z, are the same and equal to 8.38. This value results in motions with a frequency equal to the vortex-emission frequency of the static case for an angle o attack of 7^o, reported by Bobenrieth Miserda *et al.* (2004). The amplitude of the pitching motion is 4^o, resulting in a maximum angle of attack

of 9^{o} and a minimum of 5^{o}. In order to have the same maximum speed for the leading edge in both cases, the amplitude of the plunging motion is 3.49% of the chord. The computational grid is the same one used by the later referenced work.

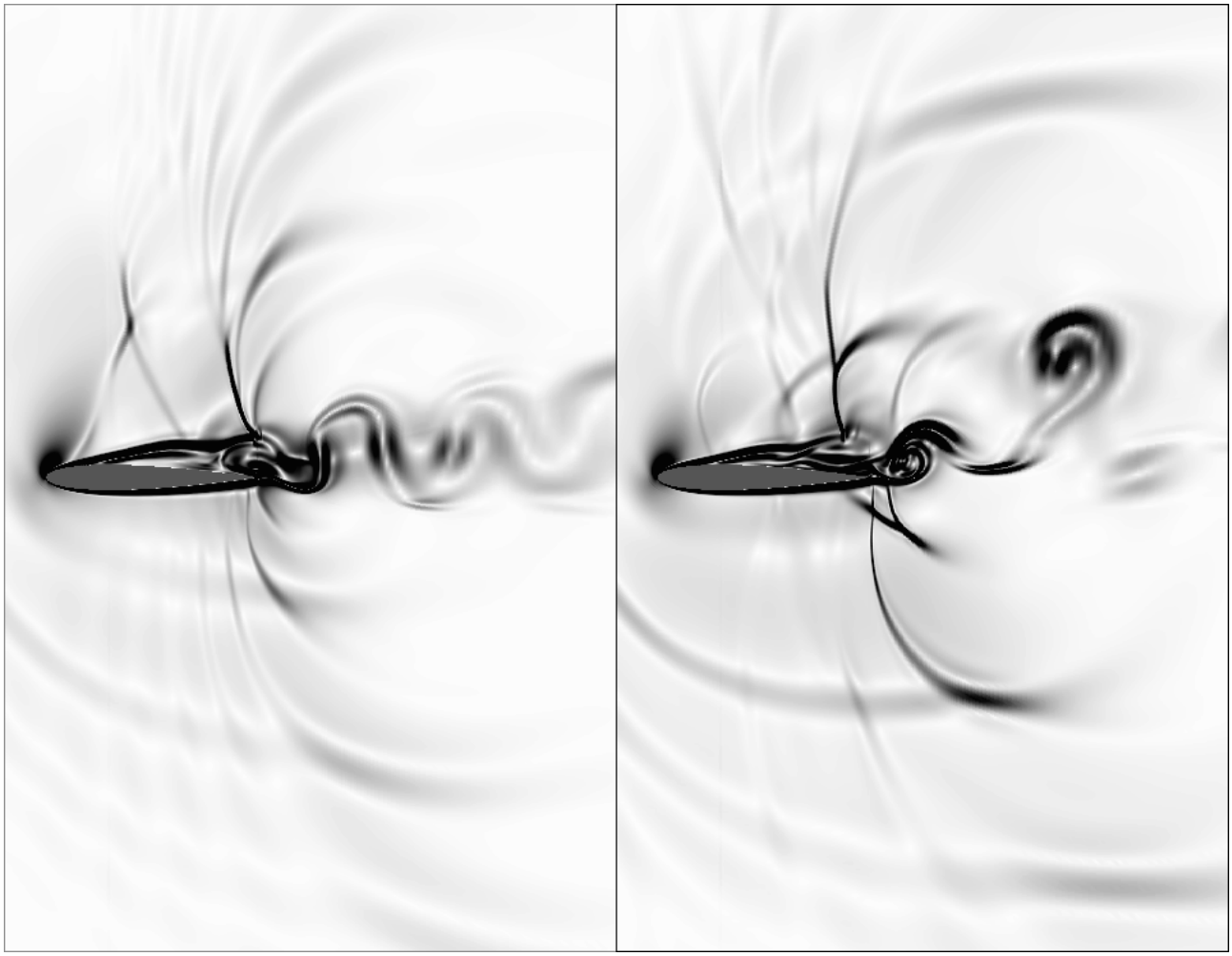

Figure 1. Visualization of pitching (left) and plunging (right) motions for the instant of maximum downward velocity of the leading edge for both cases. The variable plotted is the nondimensional magnitude of the temperature gradient. White corresponds to 0 and black corresponds to 1.5.

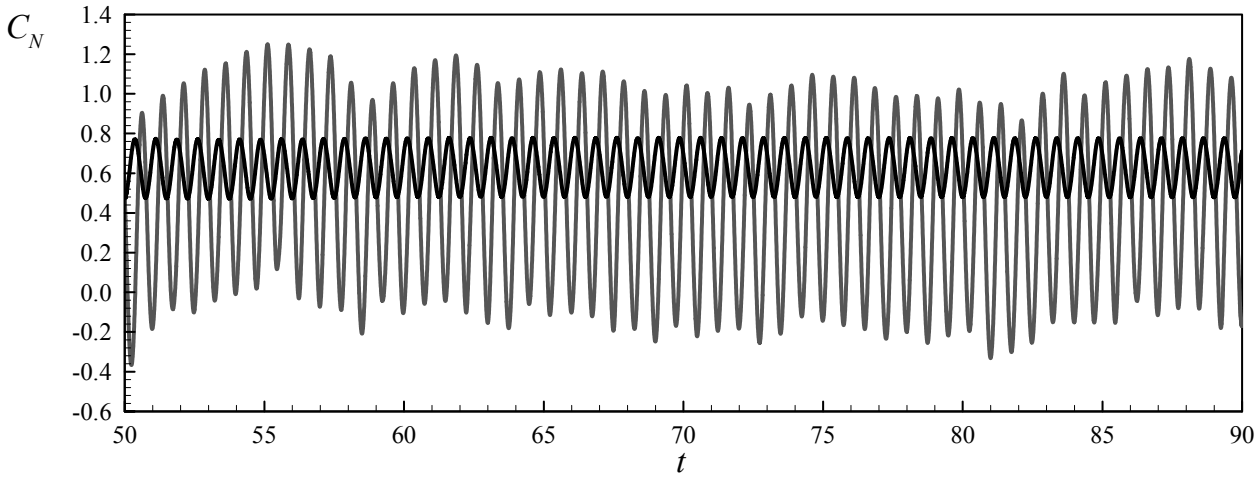

Figure 2. Unsteady normal force coefficient as a function of time. The black and gray signals correspond to the pitching and plunging motions, respectively.

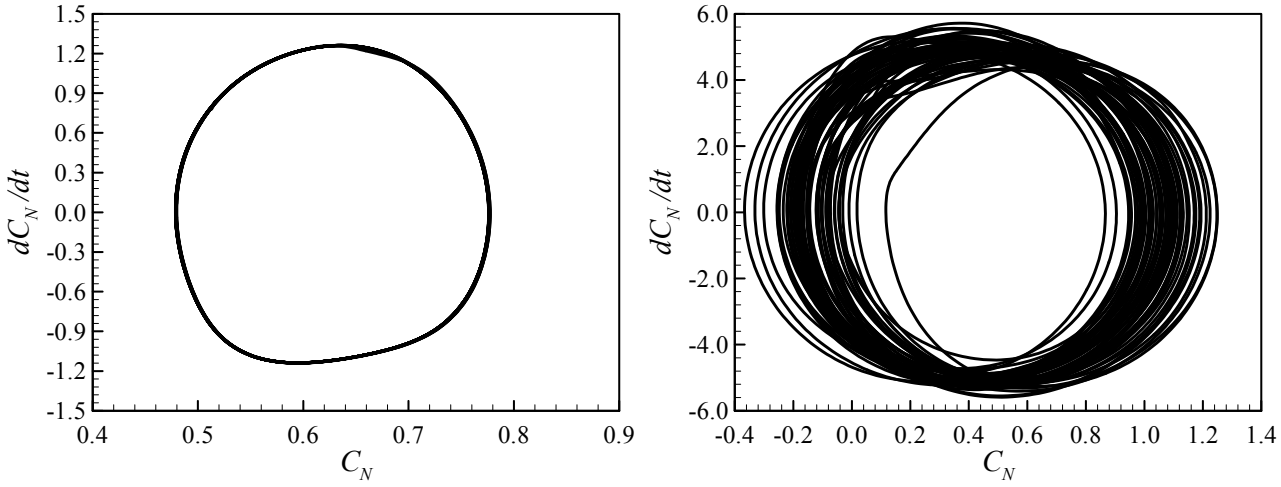

Figure 3. Phase diagram for the unsteady normal force coefficient of the pitching (left) and plunging (right) motions.

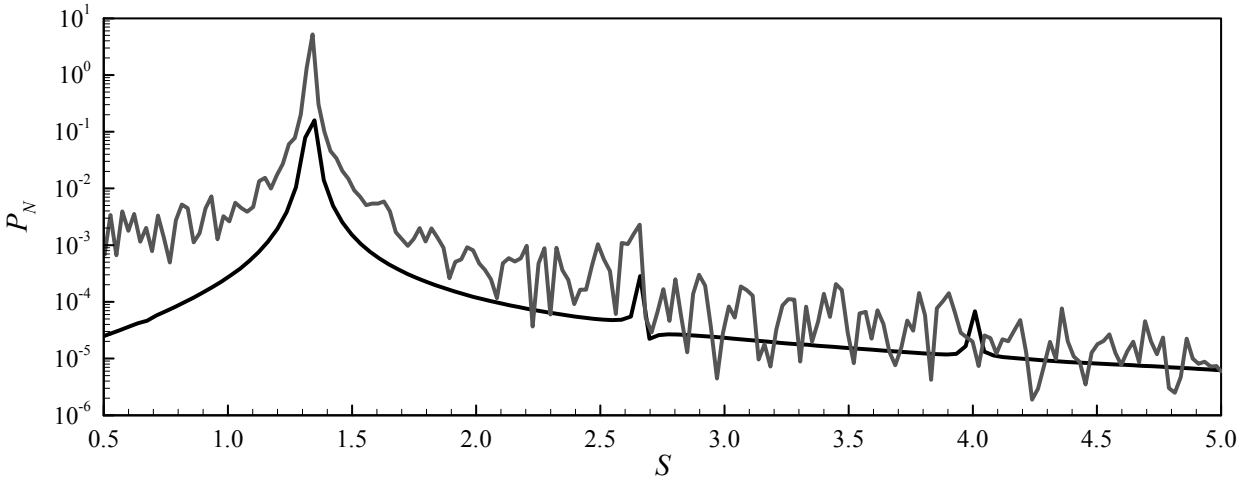

Figure 4. Power spectrum for the unsteady normal force coefficient of the pitching (black) and plunging (gray) motions.

Figure 1 shows the visualization of the pitching (left) and plunging (right) motions for the instant of maximum downward velocity of the leading edge for both cases. In both cases it is possible to observe a separated boundary layer interacting with quasi-normal shocks in the upper surface of the airfoil. This interaction results in a von Kármán vortex street for both cases. For the pitching movement, this vortex street is well defined and very regular. For the plunging movement, the vortex street is not very well defined. This difference can also be appreciated in Fig. 2 that shows the unsteady normal force coefficient as a function of time. The black signal corresponds to the pitching movement and has a very periodic behavior, associated with a very well defined vortex street. The gray signal corresponds to the pitching motion and it is possible to observe that the non-linear response of the unsteady normal force coefficient is strongly associated with a complex vortex street.

Figure 3 shows the phase diagram for the unsteady normal force coefficient of both motions. The left part corresponds to the pitching one, and reveals a very well defined phase path, resulting from a very linear behavior of the system. A non-linear response is also apparent in the phase path for the plunging motion, showed in the right part of the same figure. It is possible to observe a strong deviation generated from the temporal variation of the maximum and minimum values of the normal force coefficient, while its amplitude remains relatively constant. Figure 4 shows the power spectrum of the normal force coefficient for both cases. The black and gray lines represent the spectrum of the pitching and plunging motions, respectively. As expected, the spectrum for the pitching motion reveals a just a fundamental frequency associated with two sub-harmonics. In contrast, for the plunging motion the spectrum is broader around the fundamental frequency, and a clear definition of sub-harmonics is absent, due to the non-linear behavior of the system.

4. Conclusion

A methodology is proposed in order to simulate the laminar transonic flow around an airfoil with an imposed pitching or plunging motion. It is based on the methodology proposed by Bobenrieth Miserda and Mendonça, with the addition of pseudo-force and pseudo-work terms in the momentum and energy equations, respectively, in order to solve the system of governing equations from a non-inertial frame of reference that is moving with the airfoil. In order to make a comparison between the two types of motion, the maximum velocity of the leading edge is equal for both cases. The pitching and plunging frequencies are also the same and equal to the static vortex-emission frequency at the same angle of attack for the plunging motion and the same mean angle of attack for the pitching motion.

From a system dynamics point of view, the system response to the pitching motion is different when compared to the response to the plunging motion. For the first case, the system response is quasi-linear, with a well defined phase path associated to a power spectrum with a characteristic frequency and sub-harmonics. On the other hand, the system response to the plunging motion in a non linear one, with a phase path that is not well defined and a power spectrum that has a characteristic frequency, but with a broader distribution of energy.

These differences may be related to the level of energy associated to each type of motion. Although the maximum velocity of the leading edge is the same for both cases, in the plunging motion the whole airfoil is moving in the same direction, while in the pitching motion, if the leading edge is moving upward, the trailing edge compensates this motion moving downward. Being the energy level higher for the plunging motion, it results in a higher level of perturbations that could trigger a non-linear response from the system.

5. References

Anderson, D.A., Tannehill, J.C. and Pletcher, R.H., 1983, "Computational Fluid Mechanics and Heat Transfer", Hemisphe Publishing Corporation, New York.

Batchelor, C.K., 1983, "An Introduction to Fluid Dynamics", University Press, Cambridge.

Bobenrieth Miserda, R.F., Jalowitzki, J.R., Lauterjung Q., R. and Mendonça, A.F. de, 2004, "Numerical Simulation of the Laminar Transonic Buffet in Airfoils", 10th Brazilian Congress of Thermal Sciences and Engineering – ENCIT 2004, CIT04-0609, Rio de Janeiro, Rio de Janeiro.

Bobenrieth Miserda, R.F., Mendonça, A.F. de, 2005, "Numerical Simulation of the Vortex-Shock Interactions in a Near-Base Laminar Flow", AIAA 43rd Aerospace Sciences Meeting and Exhibit, AIAA 2005-0316, Reno, Nevada.

Hillenherms, C., Schröder, W. and Limberg, W., 2001, "Unsteady Force and Pressure Measurements on an Oscillating Rectangular Wing Section in Transonic Flow", AIAA 19th Applied Aerodynamics Conference, AIAA-2001-2468, Anaheim, California.

Krishnamurthy, R., Sarma, B.S. and Deshpande, S.M., 2004, "Kinetic Scheme for Computational Aeroelastic Analysis of 2-D Airfoils in Transonic Flows", AIAA 34th Fluid Dynamics Conference and Exhibit, AIAA 2004-2236, Portland, Oregon.

Silva, R.G.A., Mello, O.A.F. and Azevedo, J.L.F., 2004, "A Sensitivity Study of Downwash Weighting Methods for Transonic Aeroelastic Stability Analysis", AIAA 22nd Applied Aerodynamics Conference and Exhibit, AIAA 2004-5375, Providence, Rhode Island.

Tolouei, E., Mani, M., Soltani, M. R. and Boroomand, M., 2004, "Flow Analysis around a Pitching Airfoil", AIAA 22nd Applied Aerodynamics Conference and Exhibit, AIAA 2004-5200, Providence, Rhode Island.

Yee, H.C., 1997, "Explicit and Implicit Multidimensional Compact High-Resolution Shock-Capturing Methods: Formulation," Journal of Computational Physics, Vol. 131, pp. 216-232.

Zhang, Z., Yang, S. and Liu, F., 2005, "Prediction of Flutter and LCO by an Euler Method on Non-moving Cartesian Grids with Boundary-Layer Corrections", AIAA 43rdAerospace Sciences Meeting and Exhibit, AIAA 2005-833, Reno, Nevada.

6. Responsibility notice

The authors are the only responsible for the printed material included in this paper.